J. Fluid Mech. (1992), vol. 236, pp. 513–533
Printed in Great Britain

Hydrodynamic diffusion of a sphere sedimenting through a dilute suspension of neutrally buoyant spheres

By ROBERT H. DAVIS[1] AND N. A. HILL[2]

[1] Department of Chemical Engineering, University of Colorado, Boulder, CO 80309-0424, USA
[2] Department of Applied Mathematical Studies, University of Leeds, Leeds LS2 9JT, UK

(Received 17 January 1991 and in revised form 10 September 1991)

The motion of a heavy sphere sedimenting through a dilute background suspension of neutrally buoyant spheres is analysed for small Reynolds number and large Péclet number. For this particular problem, it is possible not only to calculate the mean velocity of the heavy particle, but also the variance of the velocity and the coefficient of hydrodynamic diffusivity. Pairwise, hydrodynamic interactions between the heavy sphere and the background sphere are considered exactly using volume integrals and a trajectory analysis. Explicit formulae are given for the two limiting cases when the radius of the heavy sphere is much greater and much less than that of the background spheres, and numerical results are given for moderate size ratios. The mean velocity is relatively insensitive to the ratio of the radius of the background spheres to that of the heavy sphere, unless this ratio is very large, whereas the hydrodynamic diffusivity increases rapidly as the radius ratio is increased. The predictions are in reasonable agreement with the results of falling-ball rheometry experiments.

1. Introduction

In the last two decades, considerable progress has been made in the calculation of mean settling speeds in dilute, sedimenting suspensions using renormalization techniques (e.g. Batchelor 1972, 1982; Hinch 1977; Feuillebois 1984). Of additional interest is the possibility of predicting the velocity variance and the coefficient of *hydrodynamic* diffusivity, which are measures of the fluctuations in the settling speeds of individual sedimenting particles. Hydrodynamic diffusion during batch sedimentation of nearly monodisperse suspensions has been observed experimentally by Davis & Hassen (1988), who measured the rate of spreading of the interface at the top of the suspension, and by Ham & Homsy (1988), who measured the variance in the time for a marked sphere in the interior of the suspension to fall through a given distance. It should be emphasized that the phenomenon of hydrodynamic diffusion arises from hydrodynamic interactions between particles in the suspension fluid, and is unrelated to Brownian diffusion which arises from the thermal motion of the fluid molecules surrounding each particle.

Previous theoretical studies of velocity fluctuations during the sedimentation of dilute, monodisperse suspensions include that of Caflisch & Luke (1985), who showed that an infinite velocity variance is predicted if the particles are randomly distributed in a suspension of infinite extent, and that of Koch & Shaqfeh (1991), who showed that this divergence due to long-range particle-particle interactions is

removed by a Debye-like screening mechanism which arises from three-sphere interactions causing a deficit of neighbouring particles in the vicinity of each particle. Shaqfeh & Koch (1988, 1990) have also analysed related problems involving orientational dispersion of non-spherical particles due to hydrodynamic interactions in flows of dilute suspensions.

In this paper, we consider the model problem of a single heavy sphere falling through a dilute, monodisperse suspension of neutrally buoyant spheres. This theory is directly applicable to experiments on falling-ball rheometry, in which considerable variations in the velocity of the heavy sphere have been observed (Mondy, Graham & Jensen 1986; Milliken *et al.* 1989). The significance of employing a neutrally buoyant suspension is that, in an unbounded fluid, the disturbance to the velocity field of the heavy sphere, caused by a single neutrally buoyant particle, decays like r^{-4} as the distance between their centres, r, tends to infinity. It is thus possible, in a dilute suspension, to replace ensemble averages which occur in the description of the hydrodynamic diffusivity by volume integrals over pairs of particles, without the need for complicated renormalization. Moreover, when two interacting spheres differ in size or density, they experience a relative velocity which varies as their relative position changes. In contrast, two identical spheres fall with no relative velocity, and consequently the hydrodynamic diffusivity in a monodisperse suspension cannot be calculated solely from pairwise interactions.

The paper is organized as follows. In §2 the general problem is formulated, using both a volume integral approach and a trajectory approach for averaging over pairwise interactions. Expressions for the mean velocity, the velocity variance, and the coefficient of hydrodynamic diffusion for the heavy sphere are presented. In order to make further analytical progress, the special cases when the radius of the heavy sphere is very large or small relative to that of the background spheres are addressed in §3. These limits bear some relation to the effective tracer diffusivity of molecules or very small particles flowing through a fixed bed (Koch & Brady 1985), and similarities and differences of the two problems are discussed. Numerical results for general radius ratios are also presented in §3, and the predictions are compared with data from falling-ball rheometry experiments in §4. Brief conclusions are drawn in the final section.

2. Formulation of the general problem

We consider a suspension of neutrally buoyant spheres of radius a_2 immersed in an incompressible Newtonian fluid of viscosity μ and density ρ. If the total surface area of the particles is much greater than the surface area of the walls of the container (Happel & Brenner 1973, §8.2), and provided that the heavy sphere of radius a_1 is well away from the walls, we are justified in approximating the suspension as unbounded. We shall also assume that it is 'well-mixed', i.e. the distribution of the background spheres is random and the probability distribution function for the position of the spheres' centres is statistically homogeneous over macroscopic lengthscales, i.e. lengthscales much greater than the typical distances separating the spheres. The volume fraction, c, of the neutrally buoyant background spheres is small ($c \ll 1$), but sufficiently large that hydrodynamic interactions between individual background spheres and the heavy sphere are important. The Reynolds number for the motion of particles, $Re \equiv \rho U_s a_1/\mu$, is small, so that inertial effects can be neglected. We also assume that the Péclet number, $Pe \equiv a_1 U_s/D_b$, is large, so that Brownian diffusion is weak. Here, U_s is the Stokes velocity of the heavy sphere and

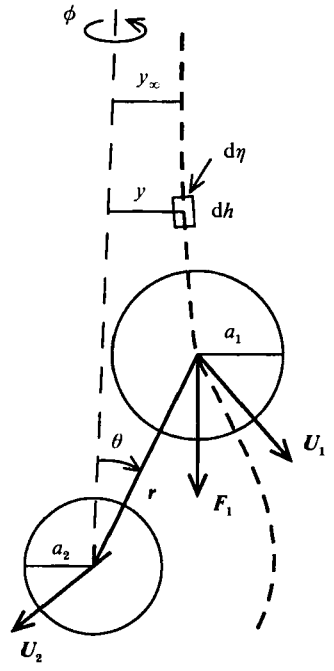

FIGURE 1. Schematic of heavy sphere and nearby background sphere.

D_b is the relative Brownian diffusivity of the two spheres. Interparticle attractive and repulsive forces are assumed negligible, and the surfaces of the spheres are considered to be ideally smooth, with the surrounding fluid treated as a continuum obeying the no-slip condition.

As the heavy sphere falls due to gravity, it encounters background spheres which slow down its motion so that the mean settling velocity of the heavy sphere is less than its Stokes velocity. The random encounters also cause the velocity of the heavy sphere to vary or fluctuate with time, giving rise to a fluctuating motion superimposed on its mean velocity. In §2.1 we show how the fluctuating motion may be analysed statistically using pairwise hydrodynamic interactions in order to predict the mean velocity, the velocity variance, and the coefficient of hydrodynamic diffusion for the heavy sphere. Before doing so, we briefly review the hydrodynamic interaction of a pair of spheres under creeping flow conditions.

Figure 1 depicts an arbitrary relative location of the heavy sphere and a background sphere. The centre of the former is at $\boldsymbol{x}_1$, and it is subject to a body force $\boldsymbol{F}_1$ due to gravity. The second sphere is neutrally buoyant ($\boldsymbol{F}_2 = 0$), with its centre at $\boldsymbol{x}_2 = \boldsymbol{x}_1 + \boldsymbol{r}$. Both spheres are torque free. Because the governing Stokes equations are linear and quasi-steady, the velocity of each sphere depends only on the instantaneous relative location of the two spheres, and is linear with respect to the applied force $\boldsymbol{F}_1$. Furthermore, the motion may be decomposed into motion along and normal to the line of centres, so that the instantaneous translational velocities of the two spheres in an otherwise quiescent and unbounded fluid may be expressed as

$$\boldsymbol{U}_1 = \frac{\boldsymbol{F}_1}{6\pi\mu a_1} \cdot \left\{ A_{11} \frac{\boldsymbol{rr}}{r^2} + B_{11} \left(\boldsymbol{I} - \frac{\boldsymbol{rr}}{r^2} \right) \right\}, \tag{2.1}$$

$$\boldsymbol{U}_2 = \frac{\boldsymbol{F}_1}{3\pi\mu(a_1 + a_2)} \cdot \left\{ A_{12} \frac{\boldsymbol{rr}}{r^2} + B_{12} \left(\boldsymbol{I} - \frac{\boldsymbol{rr}}{r^2} \right) \right\}, \tag{2.2}$$

where $\boldsymbol{I}$ is the unit second-order tensor and $r \equiv |\boldsymbol{r}|$. The mobility functions (A_{11}, A_{12}, B_{11}, and B_{12}) are as defined by Batchelor (1982) and depend on two dimensionless quantities:

$$s \equiv \frac{2r}{a_1+a_2}, \quad \lambda \equiv \frac{a_2}{a_1}.$$

Considerable research to determine these mobility functions is summarized by Jeffrey & Onishi (1984) and Kim & Karrila (1991), among others. For $s \to \infty$, $A_{11} = 1$, $B_{11} = 1$, $A_{12} = 0$, and $B_{12} = 0$, confirming that $\boldsymbol{U}_2 = 0$ and $\boldsymbol{U}_1 = \boldsymbol{U}_s$ when the spheres are widely separated, where $\boldsymbol{U}_s = \boldsymbol{F}_1/6\pi\mu a_1$ is the Stokes velocity of the heavy sphere.

2.1. *Volume-integral formulation*

Let $H(\boldsymbol{x}_1, t)$ be some property of the suspension associated with the heavy sphere centred at $\boldsymbol{x}_1$, and let $P(\boldsymbol{x}_1+\boldsymbol{r}\,|\,\boldsymbol{x}_1)$ be the probability of finding a background sphere at $\boldsymbol{x}_1+\boldsymbol{r}$, given the sphere at $\boldsymbol{x}_1$. If $H(\boldsymbol{x}_1, \boldsymbol{x}_1+\boldsymbol{r})$ is the value of H in the presence of just one other sphere at $\boldsymbol{x}_1+\boldsymbol{r}$, and if H decays more rapidly than r^{-3} as $r \to \infty$, then, as shown by Batchelor (1972), the ensemble average of H is

$$\langle H \rangle = \int H(\boldsymbol{X}_1, \boldsymbol{x}_1+\boldsymbol{r})\, P(\boldsymbol{x}_1+\boldsymbol{r}\,|\,\boldsymbol{x}_1)\, \mathrm{d}\boldsymbol{r} + O(c^2), \tag{2.3}$$

where the integral is over the whole volume of the suspension. In other words, provided that $H(\boldsymbol{x}_1, \boldsymbol{x}_1+\boldsymbol{r})$ decays more rapidly than r^{-3} as $r \to \infty$, its ensemble average $\langle H \rangle$, can be calculated to within an error of $O(c^2)$ from the volume average of H considering only the effects of the pairwise interaction between the sphere at $\boldsymbol{x}_1$ and a second sphere. If H does not decay more rapidly than r^{-3}, then the volume integral does not uniquely converge and a renormalizing quantity, whose average is known, must be found and subtracted from H so that the convergence criterion is met.

Since the disturbance in the heavy sphere's velocity, $\boldsymbol{U}_1$, from its Stokes velocity, $\boldsymbol{U}_s$, due to the presence of a single neutrally buoyant sphere decays as r^{-4}, the renormalization quantity for the mean velocity is simply $\boldsymbol{U}_s$:

$$\langle \boldsymbol{U}_1 \rangle = \boldsymbol{U}_s + n_2 \int (\boldsymbol{U}_1 - \boldsymbol{U}_s)\, p_{12}\, \mathrm{d}\boldsymbol{r} + O(c^2), \tag{2.4}$$

where $n_2 = 3c/4\pi a_2^3$ is the number density of background spheres and p_{12} is the pair distribution function defined such that $n_2 p_{12}(\boldsymbol{r}) = P(\boldsymbol{x}_1+\boldsymbol{r}\,|\,\boldsymbol{x}_1)$. In this and subsequent formulae, the angle brackets represent the ensemble average over all possible realizations of the random initial positions of the background spheres, taken after the heavy sphere has fallen a sufficient distance to undergo many encounters and establish the long-time form of the pair distribution function.

The velocity variance tensor, $\boldsymbol{V}_1$, is defined as the mean-square velocity variation of the heavy sphere from its mean velocity:

$$\boldsymbol{V}_1 \equiv \langle (\boldsymbol{U}_1 - \langle \boldsymbol{U}_1 \rangle)(\boldsymbol{U}_1 - \langle \boldsymbol{U}_1 \rangle) \rangle = \langle \boldsymbol{U}_1 \boldsymbol{U}_1 \rangle - \langle \boldsymbol{U}_1 \rangle \langle \boldsymbol{U}_1 \rangle. \tag{2.5}$$

Renormalization requires that $\langle \boldsymbol{U}_1 \rangle$ be replaced by $\boldsymbol{U}_s - O(c)$, so that for dilute suspensions the variance is given by

$$\boldsymbol{V}_1 = n_2 \int (\boldsymbol{U}_1 - \boldsymbol{U}_s)(\boldsymbol{U}_1 - \boldsymbol{U}_s)\, p_{12}\, \mathrm{d}\boldsymbol{r} + O(c^2). \tag{2.6}$$

The hydrodynamic diffusivity tensor is defined as the ensemble average of the long-time correlation function for the velocity disturbance of the heavy sphere:

$$\boldsymbol{D}_1 \equiv \left\langle \int_{-\infty}^{t} (\boldsymbol{U}_1(t') - \langle \boldsymbol{U}_1 \rangle)(\boldsymbol{U}_1(t) - \langle \boldsymbol{U}_1 \rangle)\,\mathrm{d}t' \right\rangle. \tag{2.7}$$

Using integration by parts, it may be shown that this formulation is equivalent to

$$\boldsymbol{D}_1 = \lim_{t\to\infty} \frac{1}{2}\frac{\mathrm{d}}{\mathrm{d}t}\langle (\boldsymbol{x}_1 - \langle \boldsymbol{x}_1 \rangle)(\boldsymbol{x}_1 - \langle \boldsymbol{x}_1 \rangle)\rangle, \tag{2.8}$$

where $\boldsymbol{x}_1$ is the position of the centre of the heavy sphere after time t. For dilute suspensions, renormalization again requires that $\langle \boldsymbol{U}_1 \rangle$ be replaced by $\boldsymbol{U}_s - O(c)$, so that (2.7) becomes

$$\boldsymbol{D}_1 = n_2 \int\int_{-\infty}^{t} (\boldsymbol{U}_1(t') - \boldsymbol{U}_s)(\boldsymbol{U}_1(t) - \boldsymbol{U}_s)\,\mathrm{d}t'\, p_{12}\,\mathrm{d}\boldsymbol{r} + O(c^2). \tag{2.9}$$

The pair-distribution function, $p_{12}(\boldsymbol{r})$, satisfies the Fokker–Planck equation (Batchelor 1982),

$$\frac{\partial p_{12}}{\partial t} + \boldsymbol{\nabla}\cdot(p_{12}\,\boldsymbol{V}_{12}) = 0, \tag{2.10}$$

subject to the homogeneous boundary condition of $p_{12} = 1$ as $r \to \infty$. The relative velocity of the background sphere with respect to the heavy sphere is, using (2.1) and (2.2),

$$\frac{\mathrm{d}\boldsymbol{r}}{\mathrm{d}t} = \boldsymbol{V}_{12} \equiv \boldsymbol{U}_2 - \boldsymbol{U}_1 = -\boldsymbol{U}_s \cdot \left\{ L\frac{\boldsymbol{rr}}{r^2} + M\left(\boldsymbol{I} - \frac{\boldsymbol{rr}}{r^2}\right)\right\}, \tag{2.11}$$

where the mobility functions for relative motion along and normal to the line of centres are, respectively,

$$L = A_{11} - 2A_{12}/(1+\lambda), \quad M = B_{11} - 2B_{12}/(1+\lambda).$$

2.2. *Trajectory formulation*

Although the pair-distribution function required in the volume-integral formulation may be determined using (2.10) and (2.11), in many cases it proves convenient to eliminate it by performing the integrals along trajectories which start with the spheres widely separated, where $p_{12} = 1$. To do so, we choose the volume element to be oriented along a relative trajectory, as shown in figure 1, so that $\mathrm{d}\boldsymbol{r} = y\,\mathrm{d}\phi\,\mathrm{d}h\,\mathrm{d}\eta$, where h is the coordinate along the arc of the trajectory, η is the coordinate perpendicular to the trajectory in the plane of motion, ϕ is the meridional angle about the axis of symmetry, $y = r\sin\theta$ is the horizontal separation of the spheres' centres, and θ is the angle between $\boldsymbol{r}$ and $\boldsymbol{F}_1$. Noting that $\mathrm{d}h = V_{12}\,\mathrm{d}t$, where $V_{12} \equiv |\boldsymbol{V}_{12}|$, (2.4) becomes

$$\langle \boldsymbol{U}_1 \rangle = \boldsymbol{U}_s + n_2 \int_0^{2\pi}\int_0^{\infty}\int_{-\infty}^{\infty} (\boldsymbol{U}_1 - \boldsymbol{U}_s)\, p_{12}\, V_{12}\,\mathrm{d}t\, y\,\mathrm{d}\eta\,\mathrm{d}\phi + O(c^2).$$

Moreover, the flux of particle pairs along each trajectory, $n_2 p_{12} V_{12} y\,\mathrm{d}\eta\,\mathrm{d}\phi$, is constant and equal to its value at large separations, $n_2 U_s y_\infty\,\mathrm{d}y_\infty\,\mathrm{d}\phi$, and so this becomes

$$\langle \boldsymbol{U}_1 \rangle = \boldsymbol{U}_s + n_2 U_s \int_0^{2\pi}\int_0^{\infty}\int_{-\infty}^{\infty} (\boldsymbol{U}_1 - \boldsymbol{U}_s)\,\mathrm{d}t\, y_\infty\,\mathrm{d}y_\infty\,\mathrm{d}\phi + O(c^2), \tag{2.12}$$

where the impact parameter, y_∞, is the horizontal separation of the centres of the two spheres when they are far apart. In a similar fashion, it may be shown that (2.6) and (2.9) are equivalent, respectively, to

$$\boldsymbol{V}_1 = n_2 U_s \int_0^{2\pi} \int_0^{\infty} \int_{-\infty}^{\infty} (\boldsymbol{U}_1 - \boldsymbol{U}_s)(\boldsymbol{U}_1 - \boldsymbol{U}_s)\, dt\, y_\infty\, dy_\infty\, d\phi + O(c^2), \tag{2.13}$$

$$\boldsymbol{D}_1 = \tfrac{1}{2} n_2 U_s \int_0^{2\pi} \int_0^{\infty} \int_{-\infty}^{\infty} (\boldsymbol{U}_1 - \boldsymbol{U}_s)\, dt \int_{-\infty}^{\infty} (\boldsymbol{U}_1 - \boldsymbol{U}_s)\, dt\, y_\infty\, dy_\infty\, d\phi + O(c^2). \tag{2.14}$$

In deriving (2.14), integration by parts was used.

The trajectory expressions have simple physical interpretations. The mean velocity disturbance of the heavy sphere is shown by (2.12) to equal the rate of encounters with background spheres multiplied by the mean displacement experienced per encounter. Similarly, the hydrodynamic diffusivity of the heavy sphere is shown by (2.14) to equal to one-half the rate of encounters with background spheres multiplied by the mean-square displacement per encounter. For dilute suspensions in which the encounters are uncorrelated, this is equal to the ensemble average of one-half the time rate of change of the net mean-square displacement after many encounters, which is equivalent to the common definition of a diffusion coefficient given by (2.8).

A trajectory analysis has also been used recently by Acrivos *et al.* (1992) to predict the component of the hydrodynamic diffusivity in the flow direction for a dilute suspension of neutrally buoyant particles subject to simple shear flow. They found that the dominant contribution comes from trajectories with small impact parameters.

3. Results and discussion

The calculations may be simplified considerably by taking advantage of symmetry. As noted previously, the motion of the two interacting spheres is axisymmetric, so that their centres remain in a vertical plane. This implies that the mean velocity of the heavy sphere is in the vertical direction, and that the off-diagonal components of the velocity variance and hydrodynamic diffusivity tensors are zero. Moreover, the linearity of the governing Stokes equations implies that the motion also has mirror-image symmetry about the horizontal plane in which the vector $\boldsymbol{r}$ lies when $\theta = \frac{1}{2}\pi$. This latter symmetry will be broken if the spheres come into contact, owing to surface roughness, adhesive forces, molecular slip or other effects, as discussed later. In the absence of contact, these symmetries lead to the pair-distribution function having spherical symmetry (Batchelor 1982):

$$\ln p_{12} = \int_s^{\infty} \left\{ \frac{2(L-M)}{s'L} + \frac{1}{L}\frac{dL}{ds'} \right\} ds', \quad s > 2, \tag{3.1}$$

with $p_{12} = 0$ for $s \leqslant 2$ since the spheres are not able to overlap.

The mirror-image symmetry also allows us to express the mean velocity, velocity variance and hydrodynamic diffusivity of the heavy sphere as, respectively,

$$\langle \boldsymbol{U}_1 \rangle = \boldsymbol{U}_s (1 - k_m c) + O(c^2), \tag{3.2}$$

$$\boldsymbol{V}_1 = \boldsymbol{U}_s \boldsymbol{U}_s k_v c + (U_s^2 \boldsymbol{I} - \boldsymbol{U}_s \boldsymbol{U}_s) k_h c + O(c^2), \tag{3.3}$$

$$\boldsymbol{D}_1 = \boldsymbol{U}_s \boldsymbol{U}_s \left(\frac{a_1}{U_s} \right) k_d c + O(c^2). \tag{3.4}$$

The coefficients in (3.2)–(3.4) may be calculated by either the volume integral or trajectory approach. Using (2.1) for the required disturbance velocity of the heavy sphere, together with $c = \frac{4}{3}\pi a_2^3 n_2$, yields the following expressions for the mean velocity coefficient (k_m), the horizontal velocity variance coefficient (k_h), the vertical velocity variance coefficient (k_v) and the hydrodynamic diffusivity coefficient (k_d), respectively, from the volume-integral approach:

$$k_m = \frac{(1+\lambda)^3}{8\lambda^3}\int_2^\infty (3-A_{11}-2B_{11})\,p_{12}\,s^2\,\mathrm{d}s, \tag{3.5}$$

$$k_h = \frac{(1+\lambda)^3}{40\lambda^3}\int_2^\infty (B_{11}-A_{11})^2\,p_{12}\,s^2\,\mathrm{d}s, \tag{3.6}$$

$$k_v = \frac{(1+\lambda)^3}{40\lambda^3}\int_2^\infty (2(B_{11}-A_{11})^2+15(1-B_{11})^2+10(B_{11}-A_{11})\,(1-B_{11}))\,p_{12}\,s^2\,\mathrm{d}s, \tag{3.7}$$

$$k_d = \frac{3(1+\lambda)^4}{16\lambda^3}\int_2^\infty \int_0^{\frac{1}{2}\pi}\int_{-\infty}^0 \{(B_{11}-A_{11})\cos^2\theta+(1-B_{11})\}\,\mathrm{d}\tau$$
$$[(B_{11}-A_{11})\cos^2\theta+(1-B_{11})]\,p_{12}\,s^2\sin\theta\,\mathrm{d}\theta\,\mathrm{d}s, \tag{3.8}$$

where $\tau \equiv 2U_s t/(a_1+a_2)$, with $\tau = 0$ referring to the time at which the centres of both spheres are in the horizontal plane of symmetry. The derivation of (3.8) from (2.9) requires the use of mirror-image symmetry about $\theta = \frac{1}{2}\pi$ in order to replace the upper limit of the trajectory integral with $\tau = 0$. Also, the terms in the curly brackets must be evaluated using (2.11) along the trajectory passing through the point (s,θ).

The corresponding expressions for the dimensionless coefficients from the trajectory approach are

$$k_m = \frac{3(1+\lambda)^3}{8\lambda^3}\int_0^\infty \int_{-\infty}^0 \{(B_{11}-A_{11})\cos^2\theta+(1-B_{11})\}\,\mathrm{d}\tau\sigma\,\mathrm{d}\sigma, \tag{3.9}$$

$$k_h = \frac{3(1+\lambda)^3}{16\lambda^3}\int_0^\infty \int_{-\infty}^0 \{(B_{11}-A_{11})^2\cos^2\theta\sin^2\theta\,\mathrm{d}\tau\sigma\,\mathrm{d}\sigma, \tag{3.10}$$

$$k_v = \frac{3(1+\lambda)^3}{8\lambda^3}\int_0^\infty \int_{-\infty}^0 \{(B_{11}-A_1)\cos^2\theta+(1-B_{11})\}^2\,\mathrm{d}\tau\sigma\,\mathrm{d}\sigma, \tag{3.11}$$

$$k_d = \frac{3(1+\lambda)^4}{16\lambda^3}\int_0^\infty \int_{-\infty}^0 \{(\mathrm{B}_{11}-\mathrm{A}_{11})\cos^2\theta+(1-B_{11})\}\,\mathrm{d}\tau)^2\,\sigma\,\mathrm{d}\sigma, \tag{3.12}$$

where $\sigma = 2y_\infty/(a_1+a_2)$ is the dimensionless impact parameter and uniquely defines a trajectory. Equations (3.9)–(3.12) can be shown to be identical to (3.5)–(3.8), respectively, by making the transformation $\sigma^2 = p_{12}Ls^2\sin^2\theta$ (Davis 1984). After noting that $sp_{12}^{-1}\,\mathrm{d}(p_{12}L)/\mathrm{d}s = 2(L-M)$ from Batchelor (1982), this gives

$$p_{12}\,s^2\sin\theta\,\mathrm{d}s = s\sigma\,\mathrm{d}\sigma/M\sin\theta.$$

It is also necessary to transform the trajectory integrals from τ to θ using the dimensionless components of (2.11):

$$\frac{\mathrm{d}s}{\mathrm{d}\tau} = -L\cos\theta, \quad s\frac{\mathrm{d}\theta}{\mathrm{d}\tau} = M\sin\theta, \tag{3.13a, b}$$

$$\frac{\mathrm{d}s}{\mathrm{d}\theta} = \frac{-sL\cot\theta}{M}. \tag{3.14}$$

3.1. *Asymptotic results for* $\lambda \ll 1$

When $\lambda \ll 1$, the suspension of small background spheres will reduce the mean velocity of the large heavy sphere from its Stokes velocity by behaving as an effective fluid with the Einstein viscosity correction (Batchelor 1982). The fluctuations from the mean velocity, as measured by the velocity variance and hydrodynamic diffusivity, are expected to be small.

The relevant mobility functions for $\lambda \ll 1$ are (Batchelor 1982; Fuentes, Kim & Jeffrey 1988, 1989):

$$B_{11}-A_{11} = 20\lambda^3(3s^{-4}-24s^{-6}+32s^{-8})+O(\lambda^4), \tag{3.15}$$

$$1-B_{11} = 320\lambda^3 s^{-8}+O(\lambda^4), \tag{3.16}$$

$$L = 1-3s^{-1}+4s^{-3}+\lambda(3s^{-1}-12s^{-3})+\lambda^2(-3s^{-1}+28s^{-3})+O(\lambda^3), \tag{3.17}$$

$$M = 1-\tfrac{3}{2}s^{-1}-2s^{-3}+\lambda(\tfrac{3}{2}s^{-1}+6s^{-3})+\lambda^2(-\tfrac{3}{2}s^{-1}-14s^{-3})+O(\lambda^3). \tag{3.18}$$

These expressions apply for all s except when the dimensionless separation, $s-2$, becomes small with respect to λ. From (3.17) and (3.18), it is seen that $2(L-M)/s+\mathrm{d}L/\mathrm{d}s = O(\lambda^3)$. Since from (3.1) the pair-probability function remains uniform, $p_{12} = 1+O(\lambda^3)$, it is most convenient to use the volume-integral formulation to determine the mean velocity and velocity variance of the heavy sphere. Using (3.15) and (3.16) in (3.5)–(3.7), and performing the integrations analytically, yields $k_{\mathrm{m}} = \frac{5}{2}$, $k_{\mathrm{h}} = 1747\lambda^3/48048$, and $k_{\mathrm{v}} = 157\lambda^3/546$, or

$$\langle \boldsymbol{U}_1 \rangle = \boldsymbol{U}_{\mathrm{s}}(1-\tfrac{5}{2}c)+O(c^2), \tag{3.19}$$

$$\boldsymbol{V}_1 = \frac{157}{546}\lambda^3 \boldsymbol{U}_{\mathrm{s}}\boldsymbol{U}_{\mathrm{s}}c+\frac{1747\lambda^3}{48048}(U_0^2\boldsymbol{I}-\boldsymbol{U}_{\mathrm{s}}\boldsymbol{U}_{\mathrm{s}})c+O(c^2). \tag{3.20}$$

Evaluation of the hydrodynamic diffusivity is more difficult. We start by substituting (3.17) and (3.18) into (3.14) and solving for the required relationship between s and θ along a trajectory defined by $s\sin\theta = \sigma$ for $\theta \to 0$:

$$\sin\theta = \frac{\sigma s^{\frac{1}{2}}}{(s-2)(s+1)^{\frac{1}{2}}}, \tag{3.21}$$

where terms of $O(\lambda)$ and smaller have been neglected. The hydrodynamic diffusivity may then be determined by evaluating either (3.8) or (3.12) numerically, after using (3.13*b*) to transform the trajectory variable from τ to θ. Unfortunately, the result is infinite, owing to the presence of $\xi \equiv s-2$ in the denominator of (3.21). The physical significance of this is that $M \to 0$ as $\xi \to 0$, according to (3.18) with terms of $O(\lambda)$ and smaller neglected, and so the time which the small neutrally buoyant sphere spends in near contact with the heavy sphere approaches infinity for trajectories with $\sigma \to 0$.

Koch & Brady (1985) encountered a similar divergence in their calculation of the effective diffusivity of a passive tracer flowing through a fixed bed of spheres. This divergence is overcome by weak molecular diffusion which allows the particles to diffuse away from the surface of a fixed sphere, where they have a high concentration owing to the slow flow resulting from the no-slip condition. For the current problem, the divergence may be eliminated without including this boundary-layer dispersion, because the finite size of the neutrally buoyant sphere and the torque-free condition for the heavy sphere allow them to be in relative motion, even as they approach contact. Moreover, the problem examined by Koch & Brady (1985) concerned the

diffusion of *small* particles or molecules in the presence of much larger fixed spheres, and in this sense it is more relevant to the current problem in the limit $\lambda \gg 1$, as considered in the next section. Acrivos *et al.* (1992) also encountered a divergence in their calculation of the hydrodynamic diffusion component in the flow direction for simple shear. This divergence comes from the disturbance velocity when two approaching spheres on close trajectories are far apart, and it is eliminated by a third particle disrupting the pair. The resulting leading-order contribution to the diffusivity in this case is $O(c \ln c^{-1})$.

By examining (3.17) and (3.18) for $\xi \ll 1$, it is apparent that the leading-order terms for the present problem dominate only when $\xi \gg \lambda$, and that $L = O(\lambda^2)$ and $M = O(\lambda)$ when $\xi = O(\lambda)$. As a result, the hydrodynamic diffusivity includes contributions from three regions: an outer region where $\xi = O(1)$, an inner region where $\xi = O(\lambda)$, and a middle region where $\lambda \ll \xi \ll 1$. The inner and outer regions each make a contribution of $O(\lambda^3)$ to the diffusivity, whereas the middle region makes a contribution of $O(\lambda^3 \ln \lambda^{-1})$. The last may be determined analytically by noting that the leading-order terms in the expansions of the mobility functions for $\lambda \ll \xi \ll 1$ are

$$B_{11}-A_{11} \sim -\tfrac{5}{4}\lambda^3, \quad 1-B_{11} \sim \tfrac{5}{4}\lambda^3, \quad M \sim \tfrac{3}{4}\xi, \quad L \sim \tfrac{3}{8}\xi^2, \quad \sin\theta \sim (\tfrac{2}{3})^{\frac{1}{2}}\sigma/\xi.$$

Substituting these along with (3.13*b*) in either (3.8) or (3.12), and invoking the constraint $\lambda/\alpha \leqslant \xi \leqslant \alpha$ or $\lambda/\alpha \leqslant \sigma \leqslant \alpha$, where α is small compared to unity but large compared to λ, yields

$$\left.\begin{aligned} k_{\mathrm{d}} &= \frac{25}{8}\lambda^3 \int_{\lambda/\alpha}^{\alpha}\int_0^{\pi/2}\int_0^{\pi/2} \sin^2\theta'\,\mathrm{d}\theta'\,\sin^2\theta\,\mathrm{d}\theta\frac{\mathrm{d}\xi}{\xi} + O(\lambda^3), \\ &= \frac{25\pi^2}{128}\lambda^3 \ln\lambda^{-1} + O(\lambda^3), \\ \boldsymbol{D}_1 &= \frac{25\pi^2}{128}\lambda^3 \ln\lambda^{-1}\left(\frac{a_1}{U_{\mathrm{s}}}\right) U_{\mathrm{s}}\,\boldsymbol{U}_{\mathrm{s}}\,c + O(c^2). \end{aligned}\right\} \tag{3.22}$$

The next-order terms include contributions from both the inner and outer regions, and must be evaluated numerically.

The relative mobility functions given by (3.17) and (3.18) do not account for lubrication forces and so are not valid when the dimensionless separation, $\xi = s-2$, becomes small compared to λ. In this limit, the large heavy sphere appears to the small background sphere as a nearly flat surface. The velocity field relative to this surface, due to the motion of the heavy sphere, scales as $U_{\mathrm{s}}\xi$ in the tangential direction and as $U_{\mathrm{s}}\xi^2$ in the normal direction. As a result, M is proportional to $\lambda/(\ln(\lambda/\xi)+O(1))$ and L is proportional to $\lambda\xi$. If the gap becomes very small, so that $\ln(\lambda/\xi) \gg 1$, then the small sphere effectively adheres to the surface of the large sphere. The flow around the large heavy sphere then creates a drag force of $O(\mu a_2 U_{\mathrm{s}}\lambda)$ on the small neutrally buoyant sphere. This force is transmitted via lubrication to the large sphere, causing the disturbance velocity to become $O(\lambda^2 U_{\mathrm{s}})$, rather than $O(\lambda^3 U_{\mathrm{s}})$. The drag force also causes the pair to slowly rotate, with M becoming $O(\lambda^2)$ rather than $O(\lambda)$. Provided that λ is finite, the near-contact trajectory integrals will therefore remain finite. Because of the logarithmic dependence of the transverse relative mobility function on the small gap thickness, it does not appear possible to develop analytical expressions for the contributions from the near-contact region. However, these contributions will be important only if the gap separation is allowed to become so small that $\xi \leqslant O(\lambda \mathrm{e}^{-1/\lambda})$. In the limit of $\lambda \to 0$, even

very weak non-hydrodynamic effects (such as Brownian motion, repulsive forces, and surface roughness) will prevent this possibility in practice, and we then expect the asymptotic results given by (3.19), (3.20), and (3.22) to be valid. Numerical calculations to explore this issue further are given in §3.3. In the absence of non-hydrodynamic effects, the near-contact contributions in this limit would probably be eliminated by encounters with additional small background spheres, which would disrupt the long-time interaction of the pair and pull the small neutrally buoyant sphere away from the surface of the large heavy sphere.

3.2. *Results for* $\lambda \gg 1$

For $\lambda \gg 1$, a small heavy sphere falls through a suspension of large background spheres. Expressions for the required mobility functions (A_{11}, B_{11}, L, and M) may be derived from the results of Fuentes *et al.* (1988, 1989), valid unless ξ becomes comparable to or smaller than λ^{-1}, and are found to be $1+O(\lambda^{-1})$. This implies that the small heavy sphere falls vertically with its Stokes velocity until it approaches, within a distance comparable to its own radius, the surface of a large neutrally buoyant sphere. It then slows down and begins to translate around the perimeter of the large sphere. However, it only moves a negligible distance, of $O(a_1)$, before its weight causes it to penetrate within the lubrication layer ($\xi \ll \lambda^{-1}$). Provided that the small heavy sphere starts anywhere directly above the large neutrally buoyant sphere ($y_\infty < a_2$ or $\sigma < 2$), the two will come into near contact. This is in contrast to the case of $\lambda \ll 1$, for which the small neutrally buoyant spheres follow the streamlines around the large heavy sphere, and only come into near contact for trajectories starting very close to the axis of symmetry.

When in near contact, the presence of the large neutrally buoyant sphere reduces the sedimentation velocity of the small heavy sphere to $O(\lambda^{-1} U_s)$ and so the disturbance velocity is $\boldsymbol{U}_1 - \boldsymbol{U}_s = -\boldsymbol{U}_s + O(\lambda^{-1} U_s)$, whereas $\boldsymbol{U}_1 - \boldsymbol{U}_s = O(\lambda^{-1} U_s)$ when the spheres are not in near contact. Therefore, the dominant contributions to the mean velocity, velocity variance, and hydrodynamic diffusivity for $\lambda \gg 1$ are expected to be provided by the near-contact portion of the relative trajectories. Since the magnitude of these contributions depends, in large part, on the length of time the spheres spend in near contact, we need to look carefully at the transverse relative mobility function, $M(s)$. If $\lambda \gg 1$ and $\xi \ll \lambda^{-1}$, and it is assumed for the moment that the large neutrally buoyant sphere does not rotate, then the appropriate mobility function is that given by lubrication theory for a torque-free sphere sedimenting parallel to a flat wall (Kim & Karrila 1991):

$$M \sim \frac{3}{\ln (\lambda\xi)^{-1} + O(1)}. \tag{3.23}$$

When ξ is so small that $\ln(\lambda\xi)^{-1} \gg 1$, the small sphere effectively adheres to the surface of the large sphere. The two then rotate as a pair, with the rotation rate governed by balancing the hydrodynamic torque on the large sphere from its rotation with that due to the weight of the small sphere attached to its surface:

$$8\pi\mu a_2^3 \frac{\mathrm{d}\theta}{\mathrm{d}t} = 6\pi\mu a_1 U_s a_2 \sin\theta \quad \text{or} \quad M = \frac{3}{4\lambda}. \tag{3.24}$$

By comparing (3.23) and (3.24), we see that M decreases significantly, from $O(1)$ to $O(\lambda^{-1})$, as the dimensionless separation, $\xi = s-2$, decreases from $O(\lambda^{-1})$ to $O(\lambda^{-1} \mathrm{e}^{-\lambda})$. The rate of decrease in ξ is governed by the mobility function for motion

of the small sphere toward the surface of the large sphere. From lubrication theory, this is $L = \frac{1}{2}\lambda\xi$. Using this result together with (3.23) in (3.14), and then integrating subject to the initial condition $\xi = \xi_0$ at $\theta = \theta_0$ yields

$$\frac{\sin\theta}{\sin\theta_0} = \left(\frac{\ln(\lambda\xi)^{-1}}{\ln(\lambda\xi_0)^{-1}}\right)^{3/\lambda}. \tag{3.25}$$

From this, we conclude that the change in $\sin\theta$ during the time required for $\lambda\xi$ to decrease from $O(1)$ to $O(e^{-\lambda})$ is negligible, provided that λ is sufficiently large for the condition $\lambda^{3/\lambda} - 1 \ll 1$ to be satisfied. When this is true, the small sphere adheres to the surface of the large sphere by lubrication forces for virtually the entire portion of the trajectory for which the spheres are in near contact, and so $M = 3/4\lambda$.

The trajectory analysis proves to be the most convenient for determining the mean velocity, velocity variance, and hydrodynamic diffusivity when $\lambda \gg 1$. Since the relative trajectories are vertical until near contact is reached, the initial azimuthal angle θ at the start of the near-contact portion of the trajectory is $\theta_0 = \sin^{-1}(y_\infty/a_2)$. Using (3.24) together with $\boldsymbol{U}_1 - \boldsymbol{U}_s = -\boldsymbol{U}_s + O(\lambda^{-1}\boldsymbol{U}_s)$ in (2.12) for the mean velocity from the near-contact portion of the trajectories yields

$$\begin{aligned}\langle \boldsymbol{U}_1 \rangle &= \boldsymbol{U}_s\left\{1 - \frac{4c}{a_1 a_2}\int_0^{a_2}\int_{\theta_0}^{\pi/2}\frac{\mathrm{d}\theta}{\sin\theta}\, y_\infty\, \mathrm{d}y_\infty\right\} + O(c^2)\\ &= \boldsymbol{U}_s(1 - 2\lambda c) + O(c^2).\end{aligned} \tag{3.26}$$

The velocity variance and hydrodynamic diffusivity are determined in a similar fashion using (2.13) and (2.14), respectively:

$$\boldsymbol{V}_1 = 2\lambda \boldsymbol{U}_s\, \boldsymbol{U}_s c + O(c^2), \tag{3.27}$$

$$\boldsymbol{D}_1 = \frac{16}{3}(\ln 2)\lambda^3\left(\frac{a_1}{U_s}\right)\boldsymbol{U}_s\, \boldsymbol{U}_s c + O(c^2). \tag{3.28}$$

The leading-order term for the horizontal component of the variance is only $O(\lambda^{-1})$, and includes contributions from both the near-contact and the widely separated portions of the trajectories. In contrast, the dominant contribution to the vertical component of the variance comes solely from the near-contact region. This is also true for the mean velocity disturbance and the hydrodynamic diffusivity.

In deriving (3.26)–(3.28), the mirror-image symmetry of the trajectories about the plane $\theta = \frac{1}{2}\pi$ was invoked. As discussed previously, this symmetry will be broken if the spheres come into contact because of surface roughness or discrete molecular effects. Since the predicted separation distance, when rescaled with the radius of the small heavy sphere, becomes exponentially small as λ is increased, it is anticipated that contact effects will be important in practice. One important consequence is that the horizontal components of the diffusivity will no longer be zero.

Finally, (3.28) indicates that the hydrodynamic diffusivity is very large but finite when λ is large but finite. The large value of the diffusivity arises because a small sphere and a large sphere in near-contact remain together for a long time, of $O(\lambda^2 a_1/U_s)$, and the velocity disturbance is large, of $O(U_s)$. It remains finite, however, because the weight of the small heavy sphere causes the pair to slowly rotate, until they separate at $\theta = \pi - \sin^{-1}(y_\infty/a_2)$ if lubrication forces are dominant, or at $\theta = \frac{1}{2}\pi$ if contact or repulsive forces are present to break the symmetry. The freedom of the large background spheres to rotate is a significant distinction from the behaviour of the background spheres in a fixed bed, such as in the problem studied by Koch &

Brady (1985) involving hydrodynamic diffusion of a passive tracer. In that problem, molecular diffusion is required, even when the Péclet number approaches infinity, in order to avoid a divergent result due to the tracer molecules having zero convective velocity as they approach the surface of the fixed spheres. In the current problem, the finite size of the small heavy spheres and the freedom of the large neutrally buoyant sphere to rotate allow for a finite result to be achieved in the absence of Brownian diffusion. Nevertheless, because the transverse relative mobility function M varies significantly in the lubrication boundary layer near the surface of the background sphere, it is expected that a small amount of Brownian diffusion might significantly reduce the hydrodynamic diffusivity, depending on the relative manner in which the Brownian Péclet number and the size ratio become large.

3.3. *Numerical results for* $\lambda = O(1)$

Numerical calculations were made using the trajectory analysis for $\lambda = \frac{1}{8}, \frac{1}{4}, \frac{1}{2}, 1, 2, 4$, and 8. The dimensionless coefficients for the mean velocity, velocity variance, and hydrodynamic diffusivity were calculated from (3.9)–(3.12), whereas the relative trajectories were calculated from (3.13), subject to the initial condition $s \sin\theta = \sigma$ for $\tau \to -\infty$. A second-order Euler's method was used for $s < 10$. The integrals were performed analytically for $s > 10$, using the leading-order terms in the far-field expansions.

Expressions for the required mobility functions were derived from the results of Jeffrey & Onishi (1984). For $s \gg 1$, the far-field expansions are

$$1-B_{11} = \frac{68\lambda^5}{(1+\lambda)^6 s^6} + \frac{32\lambda^3(10-9\lambda^2+9\lambda^4)}{(1+\lambda)^8 s^8} + \frac{192\lambda^5(35-18\lambda^2+6\lambda^4)}{(1+\lambda)^{10} s^{10}} + O(s^{-12}), \tag{3.29}$$

$$B_{11}-A_{11} = \frac{60\lambda^3}{(1+\lambda)^4 s^4} - \frac{60\lambda^3(8-\lambda^2)}{(1+\lambda)^6 s^6} + \frac{32\lambda^3(20-123\lambda^2+9\lambda^4)}{(1+\lambda)^8 s^8} + \frac{64\lambda^2(175+1500\lambda-426\lambda^2+18\lambda^4)}{(1+\lambda)^{10} s^{10}} + O(s^{-12}), \tag{3.30}$$

$$L = 1 - \frac{3}{(1+\lambda)s} + \frac{4(1+\lambda^2)}{(1+\lambda)^3 s^3} - \frac{60\lambda^3}{(1+\lambda)^4 s^4} + \frac{32\lambda^3(15-4\lambda^2)}{(1+\lambda)^6 s^6} - \frac{2400\lambda^3}{(1+\lambda)^7 s^7} - \frac{192\lambda^3(5-22\lambda^2+3\lambda^4)}{(1+\lambda)^8 s^8} + \frac{1920\lambda^3(1+\lambda^2)}{(1+\lambda)^9 s^9} - \frac{256\lambda^5(70-375\lambda-120\lambda^2+9\lambda^3)}{(1+\lambda)^{10} s^{10}} - \frac{1536\lambda^3(10-151\lambda^2+10\lambda^4)}{(1+\lambda)^{11} s^{11}} + O(s^{-12}), \tag{3.31}$$

$$M = 1 - \frac{3}{2(1+\lambda)s} - \frac{2(1+\lambda^2)}{(1+\lambda)^3 s^3} - \frac{68\lambda^5}{(1+\lambda)^6 s^6} - \frac{32\lambda^3(10-9\lambda^2+9\lambda^4)}{(1+\lambda)^8 s^8} - \frac{192\lambda^5(35-18\lambda^2+6\lambda^4)}{(1+\lambda)^{10} s^{10}} - \frac{16\lambda^3(560-553\lambda^2+560\lambda^4)}{(1+\lambda)^{11} s^{11}} + O(s^{-12}). \tag{3.32}$$

These expressions are accurate to three or four significant figures for $s \geqslant 3$.

In order to evaluate the far-field behaviour, it is first necessary to relate the true impact parameter, $\sigma = 2y_\infty/(a_1+a_2)$, for widely separated spheres to the dimensionless horizontal separation of the two spheres, $\sigma_0 = 2y_0/(a_1+a_2)$, when they

have reached the point at which the numerical integration is started. To do this, (3.14) is integrated subject to the initial condition $\sigma = s\sin\theta$ for $s\to\infty$ and the final condition $\sigma_0 = s_0\sin\theta_0$ at the start of the numerical integration, yielding

$$\sigma = \sigma_0 \exp\left\{-\int_{s_0}^{\infty}\frac{M-L}{sL}\,\mathrm{d}s\right\}. \tag{3.33}$$

Then, using the leading terms of (3.31) and (3.32) for $s \gg 1$ and performing the necessary expansions yields the desired result:

$$\sigma = \sigma_0\left(1-\frac{3}{2(1+\lambda)s_0}-\frac{9}{8(1+\lambda)^2 s_0^2}+\frac{5+32\lambda^2}{16(1+\lambda)^3 s_0^3}+O(s_0^{-4})\right). \tag{3.34}$$

When $\sigma \gg 1$, the heavy sphere falls past the background sphere without coming close to it, and so the far-field expansions can then be used for the entire trajectory. Using the mean velocity as an example, and substituting (3.14) and (3.29)–(3.32) into (3.9), gives

$$\begin{aligned}
&\int_{-\infty}^{0}\{(B_{11}-A_{11})\cos^2\theta+(1-B_{11})\}\,\mathrm{d}\tau \\
&\quad=\int_0^{\frac{1}{2}\pi}\{(B_{11}-A_{11})\cos^2\theta+(1-B_{11})\}\frac{s\,\mathrm{d}\theta}{M\sin\theta} \\
&\quad=\int_0^{\frac{1}{2}\pi}\left\{\frac{60\lambda^3}{(1+\lambda)^4 s^3}+\frac{90\lambda^3}{(1+\lambda)^5 s^4}+O(s^{-5})\right\}\frac{\cos^2\theta}{\sin\theta}\,\mathrm{d}\theta \\
&\quad=\frac{15\pi\lambda^3}{4(1+\lambda)^4\sigma^3}-\frac{24\lambda^3}{(1+\lambda)^5\sigma^4}+O(\sigma^{-5}).
\end{aligned} \tag{3.35}$$

In arriving at the last equation, (3.33) was expanded for $\sigma \gg 1$ and used to provide a relationship between s and θ along the trajectory. We also derived a similar expression for the far-field contributions from trajectories with $\sigma = O(1)$. Equation (3.35) may be integrated over all trajectories with $\sigma \geqslant \sigma_{\max} \gg 1$. Referring to (3.9), the contribution to the mean velocity coefficient from these trajectories is

$$\begin{aligned}
&\frac{3(1+\lambda)^3}{8\lambda^3}\int_{\sigma_{\max}}^{\infty}\int_{-\infty}^{0}\{(B_{11}-A_{11})\cos^2\theta+(1-B_{11})\}\,\mathrm{d}\tau\,\sigma\,\mathrm{d}\sigma \\
&\qquad=\frac{45\pi}{36(1+\lambda)\sigma_{\max}}-\frac{9}{2(1+\lambda)^2\sigma_{\max}^2}+O(\sigma_{\max}^{-3}),
\end{aligned} \tag{3.36}$$

indicating that the influence of the neutrally buoyant spheres on the heavy sphere decays sufficiently rapidly with distance that the final result for the mean velocity converges. The far-field contributions to the hydrodynamic diffusivity decay even more rapidly, with the final result being

$$\begin{aligned}
&\frac{3(1+\lambda)^4}{16\lambda^3}\int_{\sigma_{\max}}^{\infty}\left(\int_{-\infty}^{0}\{(B_{11}-A_{11})\cos^2\theta+(1-B_{11})\}\,\mathrm{d}t\right)^2\sigma\,\mathrm{d}\sigma \\
&\qquad=\frac{675\pi^2\lambda^3}{1024(1+\lambda)^4\sigma_{\max}^4}-\frac{27\pi\lambda^3}{4(1+\lambda)^5\sigma_{\max}^5}+O(\sigma_{\max}^{-6}).
\end{aligned} \tag{3.37}$$

Similar far-field expressions may also be derived for the velocity variance.

λ	$\frac{1}{8}$	$\frac{1}{4}$	1	1	2	4	8
b_1	0.9942	0.9729	0.9272	0.8905	0.7642	0.4734	0.2377
b_2	1.536	3.843	5.611	5.772	5.020	3.710	2.704
b_3	−1.544	0.3421	4.404	7.070	5.604	1.894	−0.840
d_1	0.99968	0.9951	0.9537	0.7750	0.4768	0.2488	0.1250
d_2	−0.00018	0.0088	0.1514	0.9306	2.277	3.610	5.620
d_3	−0.003	−0.026	−0.194	−0.900	−2.188	−4.061	−8.500
d_4	0	0	−0.3	−2.0	−4.5	−6.4	−9.2
e_1	1.518	3.795	5.600	6.043	5.600	3.795	1.518
e_2	−1.536	0.323	4.179	6.327	4.179	0.323	−1.536
L_1	0.3025	0.6040	1.173	2.000	2.788	3.759	5.658
L_2	−0.458	−0.679	−1.115	−1.800	−2.649	−4.224	−8.557
L_3	0.356	−0.320	−1.63	−4.000	−5.17	−6.48	−9.16
M_0	0.0108	0.0596	0.2142	0.4021	0.4077	0.2451	0.1148
M_1	0.721	1.391	2.274	2.967	3.352	3.097	2.602
M_2	−0.396	0.440	2.750	5.088	4.777	1.918	−0.696

TABLE 1. Values of constants that appear in the near-field expressions for the mobility functions (3.38)–(3.41)

λ	$\frac{1}{8}$	$\frac{1}{4}$	$\frac{1}{2}$	1	2	4	8
k_m	2.69	2.65	2.61	2.52	2.47	2.78	4.20
	(—)	(2.56)	(2.53)	(2.52)	(2.44)	(2.66)	(—)
k_h	1.14×10^{-4}	4.44×10^{-4}	2.60×10^{-3}	1.97×10^{-3}	4.95×10^{-2}	5.24×10^{-2}	3.66×10^{-2}
k_v	1.15×10^{-3}	6.18×10^{-3}	2.99×10^{-2}	0.127	0.381	0.955	2.66
k_d	0.023	0.085	0.341	1.33	5.16	26.0	220

TABLE 2. Numerical results for the dimensionless coefficients for the mean velocity disturbance, the horizontal and vertical velocity variance, and the hydrodynamic diffusivity. The results in parentheses are from Batchelor & Wen (1982).

For $\xi \equiv s-2 \ll 1$, the near-field expansions are

$$A_{11} = d_1 + d_2\xi + d_3\xi^2 \ln\xi^{-1} + d_4\xi^2 + O(\xi^3(\ln\xi^{-1})^2), \tag{3.38}$$

$$B_{11} = \frac{b_1(\ln\xi^{-1})^2 + b_2\ln\xi^{-1} + b_3}{(\ln\xi^{-1})^2 + e_1\ln\xi^{-1} + e_2} + O(\xi(\ln\xi^{-1})^3), \tag{3.39}$$

$$L = L_1\xi + L_2\xi^2\ln\xi^{-1} + L_3\xi^2 + O(\xi^3(\ln\xi^{-1})^2), \tag{3.40}$$

$$M = \frac{M_0(\ln\xi^{-1})^2 + M_1\ln\xi^{-1} + M_2}{(\ln\xi^{-1})^2 + e_1\ln\xi^{-1} + e_2} + O(\xi(\ln\xi^{-1})^3. \tag{3.41}$$

The various coefficients in these expressions are functions of λ, and are tabulated in table 1, using results from Jeffrey & Onishi (1984), with additional significant figures kindly provided by David Jeffrey (personal communication). The near-field expression for L is accurate to three or four significant figures for $\xi \leqslant 0.015$, whereas the near-field expressions for $B_{11}-A_{11}$, $1-B_{11}$, and M are accurate to two or three significant figures for $\xi \leqslant 0.015$, with the accuracy decreasing as λ decreases.

In carrying out the numerical integrations, the far-field expressions for the mobility functions were used for $s \geqslant 3$, whereas the near-field expressions were used for $s \leqslant 2.015$. For $2.015 < s < 2.1$, the near-field results were multiplied by a correction factor found from interpolating the exact numerical results reported by

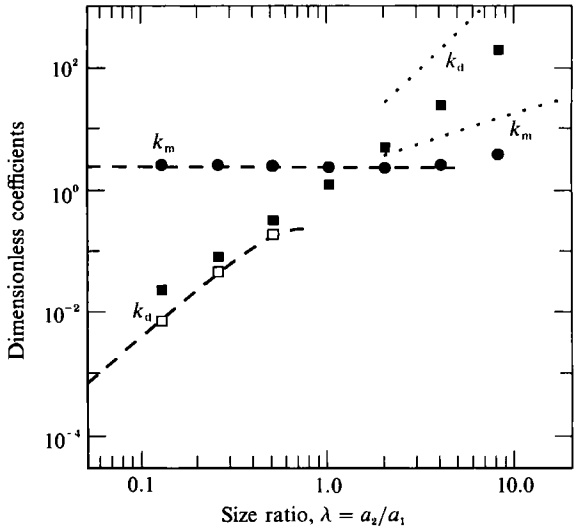

FIGURE 2. The dimensionless coefficients for the mean disturbance velocity (k_m) and the hydrodynamic diffusivity (k_d) of the heavy sphere as a function of the size ratio. The symbols are numerical results, the dashed lines are the asymptotic results for $\lambda \ll 1$, and the dotted lines are the asymptotic results for $\lambda \gg 1$.

Jeffrey & Onishi (1984), whereas the far-field results were multiplied by a correction factor found in a similar manner for $2.1 \leqslant s < 3$. For $\lambda < 1$, additional exact values of the mobility functions were obtained from a series expansion. The final results for k_m, k_v, k_h, and k_d are shown in table 2. The values for k_m are within a few percent of the results previously computed by Batchelor & Wen (1982) using the pair-distribution function and a volume integral approach. The numerical results are also shown in figures 2 and 3, together with the asymptotic results for $\lambda \ll 1$ and $\lambda \gg 1$. The numerical values for small λ are in reasonable agreement with the asymptotic results. However, the numerical values for the velocity variance and hydrodynamic diffusivity do not decrease as rapidly with decreasing λ as predicted by the asymptotic theory. The difference is due to the near-contact contributions to the numerical calculations. Additional calculations were made for which it was assumed that a non-hydrodynamic effect, such as surface roughness, prevents the particles from coming closer than some small dimensionless separation distance, ξ_c. Assuming that the transverse mobility remains at the value given by the hydrodynamic formula for this separation, it was found that good agreement with the asymptotic formulae for small λ could be obtained by choosing $\xi_c = O(10^{-3})$–$O(10^{-2})$. The open symbols in figures 2 and 3 are the results of these calculations for $\xi_c = 10^{-2}$.

For large λ, the general trends predicted by the asymptotic theory are observed (k_d proportional to λ^3, k_m and k_v proportional to λ, and k_h proportional to λ^{-1}), but even $\lambda = 8$ is not large enough to give quantitative agreement. This is as expected, since the condition $\lambda^{3/\lambda} - 1 \ll 1$ is not met, and so the transverse relative mobility function for a significant portion of each near-contact trajectory is larger than given by (3.24). Performing numerical calculations for larger λ is not practical, because typical separations then become smaller than molecular distances.

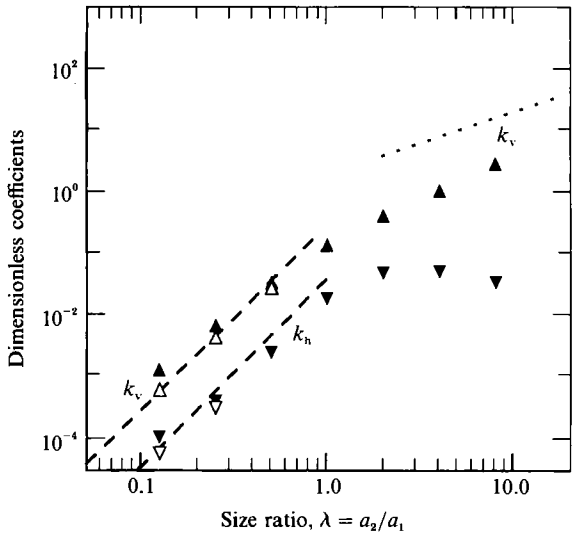

FIGURE 3. The dimensionless coefficients for the vertical velocity variance (k_v) and the horizontal velocity variance (k_h) of the heavy sphere as a function of the size ratio. The symbols are numerical results, the dashed lines are the asymptotic results for $\lambda \ll 1$, and the dotted lines are the asymptotic results for $\lambda \gg 1$.

4. Comparison with falling-ball experiments

Falling-ball rheometry is a technique used to study neutrally buoyant suspensions of non-colloidal particles. The common procedure is to drop a heavy sphere along the centreline of a cylindrical vessel containing a viscous fluid in which neutrally buoyant particles are suspended. An effective viscosity is calculated as the ratio of the Stokes velocity of the heavy sphere (corrected for wall effects) to its observed mean fall velocity. The average fall velocity for each experiment is determined by measuring the time for the heavy sphere to fall a given vertical distance. Since considerable variation in this average velocity is observed, each experiment is repeated several times. The data are then reported as either the mean velocity or the effective viscosity together with its 95% confidence limits, for each set of repeated experiments. Here, we compare this information with our predictions for the mean velocity and the hydrodynamic diffusivity (it is not possible to determine the velocity variance from the reported experiments, since only the average vertical velocity over a given fall distance was measured – and not the instantaneous velocity of the heavy sphere).

Most falling-ball experiments have been carried out with suspensions that are either concentrated or contain rod-like background particles. However, Milliken *et al.* (1989) performed experiments with spheres having several size ratios and which included one moderately dilute concentration ($c = 0.05$). Their data, taken from the first row of table 2 of their paper, are given in table 3. The suspending fluid had viscosity $\mu = 120$ g cm^{-1} s^{-1} and density $\rho = 1.18$ g cm^{-3}. The neutrally buoyant spheres had a fixed radius of $a_2 = 0.159$ cm. The falling balls had nominal densities of 8.3–8.7 g cm^{-3}. The information necessary to determine the indicated Stokes velocities, corrected for wall effects, was kindly provided by Robert Powell (personal communication). The uncertainties shown for the mean velocities represent the 95% confidence limits, equal to $\sigma_u t_{0.025}/n^{\frac{1}{2}}$, where σ_u is the standard deviation of fall velocities, n is the number of measurements ($n = 10$ for all experiments, except

λ	0.200	0.333	0.500	1.000	1.333	2.000
a_1 (cm)	0.794	0.476	0.318	0.159	0.119	0.079
U_s (cm s^{-1})	6.532	2.616	1.216	0.3238	0.1870	0.0855
$\langle U_1 \rangle$ (cm s^{-1})	5.70 ± 0.039 (5.66)	2.26 ± 0.021 (2.27)	1.097 ± 0.0017 (1.06)	0.2858 ± 0.0079 (0.283)	0.1535 ± 0.0054 (0.164)	0.0717 ± 0.0011 (0.07949)
D_1 (cm^2 s^{-1})	2.7 ± 10^{-3} (1.4×10^{-2})	2.0×10^{-3} (9.4×10^{-3})	2.7×10^{-3} (6.6×10^{-3})	2.2×10^{-3} (3.4×10^{-3})	3.1×10^{-3} (2.6×10^{-3})	1.8×10^{-4} (1.7×10^{-3})
D_b (cm^2 s^{-1})	2.3×10^{-17}	1.6×10^{-17}	5.7×10^{-17}	1.1×10^{-16}	1.5×10^{-16}	2.3×10^{-16}
k_m	2.6 ± 0.1 (2.66)	2.7 ± 0.2 (2.63)	2.0 ± 0.3 (2.61)	2.4 ± 0.5 (2.52)	2.8 ± 0.6 (2.49)	3.2 ± 0.3 (2.47)
k_d	0.010 (0.056)	0.032 (0.15)	0.14 (0.34)	0.86 (1.33)	2.9 (2.33)	0.55 (5.16)

TABLE 3. Experimental values for the mean velocity and hydrodynamic diffusivity, adapted from the data of Milliken *et al.* (1989). The corresponding numerical predictions from the theory are shown in parentheses.

$n = 15$ for $\lambda = 1.333$), $t_{0.025} = 2.26$ for $n = 10$, and $t_{0.025} = 2.14$ for $n = 15$. The diffusivity of the heavy sphere in the vertical direction due to encounters with the neutrally buoyant spheres is then given by

$$D_1 = \frac{\sigma_u^2 H}{2\langle U_1 \rangle}, \tag{4.1}$$

where H is the fall distance ($H = 10$ cm for these experiments). This equation follows from the definition $D_1 = \sigma_h^2/2t$, which is equivalent to (2.8), together with the transformations $\sigma_u = \sigma_h/t$ and $t = H/\langle U_1 \rangle$ to account for the experiments being performed with fixed fall distances rather than fixed fall times.

The experimental values of the mean velocity and the hydrodynamic diffusivity are compared with theoretical predictions in table 3. Using the definitions (3.2) and (3.4), the dimensionless coefficients for the mean velocity (k_m) and hydrodynamic diffusivity (k_d) were also determined and are listed in table 3. The predicted mean velocities are in good agreement with the measurements, and the coefficient for the mean velocity is relatively insensitive to the size ratio over the range studied. The predicted hydrodynamic diffusivities are comparable to the measured diffusivities for size ratios near unity, but are higher than the measurements by a factor of five for $\lambda = 0.2$ and $\lambda = 0.33$, and by a factor of ten for $\lambda = 2$. Unfortunately, the number of repeated measurements is too small to rule out uncertainty in the standard deviations as a major source of the disagreement in the diffusivities. Another possible explanation for the discrepancy for small λ is that the correlation times were reduced because the large falling sphere at $c = 0.05$ and $\lambda < 1$ had several background spheres, rather than a single one, at a given time within a distance comparable to its own radius. The suspension would need to be more dilute for only pairwise encounters to dominate the diffusivity. In addition, small surface roughness or other effects may have prevented close contact and thus reduced the diffusivity. Surface roughness may also have reduced the diffusivity for $\lambda = 2$, but not by the factor of ten observed. The Brownian diffusivities of the falling ball are also listed in table 3, and these are clearly negligible.

5. Concluding remarks

The mean velocity, velocity variance, and hydrodynamic diffusivity have been predicted for a heavy sphere falling under creeping flow conditions through a dilute suspension of neutrally buoyant spheres. The pairwise additivity theory for the mean velocity and the velocity variance requires that the typical separation distance of the background spheres be large compared to their radius, implying that $c \ll 1$. The theory for the hydrodynamic diffusivity has the additional requirement that the typical separation of the background spheres is large compared to the radius of the heavy sphere, so that the heavy sphere encounters only one background sphere at a time. Thus, both $c \ll 1$ and $c \ll \lambda^3$ must be satisfied. Further progress for non-dilute suspensions may be made in the future by numerical simulations (Mondy, Ingber & Dingman 1991).

The results for the mean velocity are in good agreement with the earlier theory of Batchelor & Wen (1988). The new results for the velocity variance and hydrodynamic diffusivity describe the fluctuations in the settling velocity of the heavy sphere as it undergoes close encounters with the background spheres. These velocity fluctuations are correlated over timescales comparable to the duration of an encounter, provided

that the suspension is sufficiently dilute. For dilute suspensions, the mean velocity disturbance, the velocity variance, and the hydrodynamic diffusivity of the heavy sphere are all proportional to the concentration of background spheres, owing to the pairwise nature of the interactions. This is in contrast to the expected behaviour for monodisperse suspensions, in which two interacting spheres sediment at the same velocity and must encounter a third particle for their motion to become uncorrelated. In fact, Koch & Shaqfeh (1991) predict that long-range hydrodynamic interactions cause the hydrodynamic diffusivity to increase with decreasing concentration. Experiments with nearly monodisperse suspensions by Davis & Hassen (1988) and Ham & Homsy (1988) gave hydrodynamic diffusivities of $O(aU_s)$ which increase with increasing concentration for dilute suspensions, reach a maximum at a concentration of only a few percent by volume, and then decrease with further concentration increases. It may be that the initial increase at low concentrations is due to a change in mechanism from pairs separating due to the small differences in particle sizes to pairs separating because of encountering a third particle. When all the particles are settling, there is a large contribution to the hydrodynamic diffusivity from long-range interactions that are not present when only one sphere is settling and the rest are neutrally buoyant. For comparison, the available results for $\lambda = 1$ and $c = 0.05$ give a diffusivity of approximately $5aU_s$ for the former case and only $0.05aU_s$ for the latter.

The mean velocity is shown to be nearly independent of the size ratio of the neutrally buoyant spheres to the heavy sphere, provided that this ratio is less than about four. For larger size ratios, the mean velocity of the heavy sphere is predicted to decrease, primarily because lubrication forces cause it to maintain near contact with a neutrally buoyant sphere for a long duration. These short-range hydrodynamic forces were not included in the recent theory by Brenner *et al.* (1990), and so they predicted that the effective viscosity would be independent of the size ratio. Falling-ball rheometry experiments for $c = 0.05$ confirm this prediction for small and moderate size ratios. Unfortunately, data for dilute suspensions of neutrally buoyant spheres that are much larger than the falling ball are not available in the literature. For highly concentrated suspensions ($c \geqslant 0.5$), however, Milliken *et al.* (1989) have observed that the mean velocity increases (effective viscosity decreases) as the size ratio increases. This is thought to be due to the ability of a small heavy sphere to pass more easily through the spaces between the neutrally buoyant spheres, a mechanism that is not important for dilute suspensions.

The hydrodynamic diffusivity coefficient is shown to increase dramatically with increasing size ratio of the neutrally buoyant spheres to the falling sphere, approximately as the cube of this ratio. As a result, the dimensional hydrodynamic diffusivity of the falling sphere depends strongly on the size of the neutrally buoyant spheres, but only weakly on its own size. These trends are confirmed by the falling-ball rheometry data for small and moderate size ratios. For large size ratios, the behaviour is dominated by lubrication forces which cause the near-contact interactions to have long correlation times. The results are very sensitive to the magnitude of the transverse relative mobility function. Since this function depends strongly on the small distance separating the two interacting spheres, it is anticipated that small surface roughness elements, or weak Brownian or repulsive forces, may cause significant changes in the final results. In order that the Brownian motion of the falling sphere is small compared to its hydrodynamic diffusion, the requirement $D_1/D_b = k_d a_1 U_s c/D_b \gg 1$ must be met, where $D_b = kT/6\pi\mu a_1$ for dilute suspensions, $U_s = 2a_1^2|\rho_1 - \rho|g/9\mu$, $k = 1.381 \times 10^{-16}$ erg K^{-1} is the Boltzmann con-

stant, T is the absolute temperature, and g is the gravitational acceleration. For typical suspensions ($T = 300$ K, $g = 981$ cm s^{-2}, $|\rho_1 - \rho| = 0.01$ g cm^{-3}, $c = 0.01$), the results of the present work may be used to show that the Brownian diffusivity of the heavy particle is smaller than the vertical component of the hydrodynamic diffusivity when its radius and the radius of the neutrally buoyant spheres both exceed 3.5 μm. This bound will be reduced if the volume fraction of background spheres or the density difference between the heavy sphere and the fluid is increased. Of course, the present theory does not provide a non-zero value for the horizontal component of the hydrodynamic diffusivity, as this requires higher-order interactions between three or more particles or the presence of effects such as surface roughness, repulsion, or inertia which would break the symmetry of the relative trajectories.

We wish to thank John Hinch and Eric Shaqfeh for several enlightening discussions, David Jeffrey and Robert Powell for numerical and experimental data, and the National Science Foundation and the National Aeronautics and Space Administration for financial support. A portion of this work was also undertaken while R. H. D. was visiting the Massachusetts Institute of Technology, with support from the Guggenheim Foundation.

REFERENCES

Acrivos, A., Batchelor, G. K., Hinch, E. J. & Mauri, R. 1992 Longitudinal shear-induced diffusion of spheres in a dilute suspension. *J. Fluid Mech.* (submitted).

Batchelor, G. K. 1972 Sedimentation in a dilute dispersion of spheres. *J. Fluid Mech.* **52**, 269–272.

Batchelor, G. K. 1982 Sedimentation in a dilute polydisperse system of interacting spheres. Part 1. General theory. *J. Fluid Mech.* **119**, 379–408.

Batchelor, G. K. & Wen, C.-S. 1982 Sedimentation in a dilute polydisperse system of interacting spheres. Part 2. Numerical results. *J. Fluid Mech.* **124**, 495–528.

Brenner, H., Graham, A. L., Abbott, J. R. & Mondy, L. A. 1990 Theoretical basis for falling-ball rheometry in suspensions of neutrally buoyant spheres. *Intl J. Multiphase Flow* **16**, 579–596.

Caflisch, R. E. & Luke, J. H. C. 1985 Variance in the sedimentation speed of a suspension. *Phys. Fluids* **28**, 759–760.

Davis, R. H. 1984 The rate of coagulation of a dilute polydisperse system of sedimenting spheres. *J. Fluid Mech* **145**, 179–199.

Davis, R. H. & Hassen, M. A. 1988 Spreading of the interface at the top of a slightly polydisperse sedimenting suspension. *J. Fluid Mech.* **196**, pp. 107–134. Corrigendum *J. Fluid Mech.* **202** (1989), 598–599.

Feuillebois, F. 1984 Sedimentation in a dispersion with vertical inhomogeneities. *J. Fluid Mech.* **139**, 145–171.

Fuentes, Y. O., Kim, S. & Jeffrey, D. J. 1988 Mobility functions for two unequal viscous drops in Stokes flow. I. Axisymmetric motions. *Phys. Fluids* **31**, 2445–2455.

Fuentes, Y. O., Kim, S. & Jeffrey, D. J. 1989 Mobility functions for two unequal viscous drops in Stokes flow. II. Asymmetric motions. *Phys. Fluids* A **1**, 61–76.

Ham, J. M. & Homsy, G. M. 1988 Hindered settling and hydrodynamic dispersion in quiescent sedimenting suspensions. *Intl J. Multiphase Flow* **14**, 533–546.

Happel, J. & Brenner, H. 1973 *Mechanics of Fluids and Transport Processes*, 2nd revised edn. Martinus Nijhoff.

Hinch, E. J. 1977 An averaged-equation approach to particle interactions in a fluid suspension. *J. Fluid Mech.* **83**, 695–720.

Jeffrey, D. J. & Onishi, Y. 1984 Calculation of the resistance and mobility functions for two unequal rigid spheres in low-Reynolds-number flow. *J. Fluid Mech.* **139**, 261–290.

KIM, S. & KARRILA, S. J. 1991 *Microhydrodynamics: Principles and Selected Applications.* Butterworth-Heinemann.

KOCH, D. L. & BRADY, J. F. 1985 Dispersion in fixed beds. *J. Fluid Mech.* **154**, 399–427.

KOCH, D. L. & SHAQFEH, E. S. G. 1991 Screening in sedimenting suspensions. *J. Fluid Mech.* **224**, 275–303.

MILLIKEN, W. J., MONDY, L. A., GOTTLIEB, M., GRAHAM, A. L. & POWELL, R. L. 1989 The effect of the diameter of falling balls on the apparent viscosity of suspensions of spheres and rods. *PhysicoChem. Hydrodyn.* **11**, 341–355.

MONDY, L. A., GRAHAM, A. L. & JENSEN, J. L. 1986 Continuum approximations and particle interactions in concentrated suspensions. *J. Rheol.* **30**, 1031–1051.

MONDY, L. A., INGBER, M. S. & DINGMAN, S. E. 1991 Boundary element method simulations of a ball falling through quiescent suspensions. *J. Rheol.* (submitted).

SHAQFEH, E. S. G. & KOCH, D. L. 1988 The effect of hydrodynamic interactions on the orientation of axisymmetric particles flowing through a fixed bed of spheres or fibers. *Phys. Fluids* **31**, 728–743.

SHAQFEH, E. S. G. & KOCH, D. L. 1990 Orientational dispersion of fibers in extensional flows. *Phys. Fluids* A**2**, 1077–1093.